

199
PROGRESS REPORT NO. 30-16

**DEVELOPMENT OF A MINIATURE ACCELEROMETER
WITH A FUSED-QUARTZ SUSPENSION**

A. R. JOHNSTON

FACILITY FORM 802

N 64 847 50

(ACCESSION NUMBER)

19
(PAGES)

(NASA CR OR TMX OR AD NUMBER)

(THRU)

None
(CODE)

(CATEGORY)

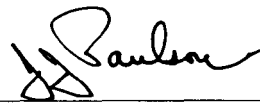
**JET PROPULSION LABORATORY
CALIFORNIA INSTITUTE OF TECHNOLOGY
PASADENA, CALIFORNIA
OCTOBER 1, 1959**

National Aeronautics and Space Administration
Contract No. NASw-6

Progress Report No. 30-16

**DEVELOPMENT OF A MINIATURE ACCELEROMETER
WITH A FUSED-QUARTZ SUSPENSION**

A. R. Johnston



J. Paulson, *Chief*
Electromechanical Development Section

Copy No. JL 44

JET PROPULSION LABORATORY
California Institute of Technology
Pasadena, California
October 1, 1959

**Copyright © 1959
Jet Propulsion Laboratory
California Institute of Technology**

CONTENTS

	Page
I. Introduction	1
II. Design and Construction	4
A. Suspension	4
B. Pickoff	6
C. Magnetic Circuit	7
D. Parts and Assembly	8
E. Amplifier	9
III. Experimental Data	11
IV. Conclusions	15
References	16
Acknowledgements	16

TABLE

1. Data From Short-Term Stability Test, Used to Determine Scale Factor, Null Offset and Null Angle	12
--	----

FIGURES

1. Diagramatic View of Accelerometer	2
2. Fused-Quartz Suspension	4
3. Two Photographic Views of the Suspension	5
4. View of Quartz-Working Area	6
5. Suspension Fabrication Jig	7
6. Diagramatic View Showing the Pickoff Elements	7
7. Output of Pickoff Photodiodes, a and b, as a Function of Pendulum Position	7
8. Sketch of Magnetic Circuit	8
9. Exploded View of Mechanical parts	8
10. Assembled Accelerometer	9
11. Schematic of Servo Amplifier Used in Testing	9
12. Experimental Phase and Gain vs Frequency of Amplifier	10
13. Block Diagram of the Force-Balance Loop, Including Design Parameters	10
14. Output Current From Amplifier in 1K Load vs Pendulum Angle, Open Loop	11
15. Null Offset and Scale Factor as Function of Null Angle	13
16. Null Angle and Scale Factor as Function of Temperature, for Elevated Temperature	13
17. 1 g Linearity Test of Two Suspensions	13
18. Data From Centrifuge Test	14

ABSTRACT

A miniature accelerometer has been constructed which employs a fused-quartz torsion fiber suspension. The purpose was to demonstrate a small yet reasonably accurate component, and at the same time explore the possibilities of fused quartz in a specific application. The accelerometer is based on the well-known force-balance servo principle, and employs a photoelectric pickoff. The design and construction of the device are described.

Complete tests have been performed on two suspensions, including centrifuge tests. The results are included. An rms value for null uncertainty or variation in null offset of $\pm 1/2 \times 10^{-4} g$ was observed, and linearity error to 1 g of averaging $\pm 3/4 \times 10^{-4} g$ rms was observed.

It appears that the torsion fiber suspension can provide a stable support with extremely low uncertainty torques, although control of the low frequency transverse resonance may be necessary if operation in a severe vibration environment is contemplated. The range of full-scale acceleration values which can be realized is discussed.

I. INTRODUCTION

There are two main purposes of the miniature accelerometer project. One is to demonstrate an accelerometer of unusually small size which still maintains enough accuracy to be useful for inertial guidance. A second is to explore the capability of fused quartz in a specific application. An important part of the work to date has been the development of technique to successfully fabricate such an instrument. The suspension and pickoff, in particular, required new technique. The advantages of small size in such an instrument are obvious and hardly need emphasizing here. If both gyros and accelerometers are available in miniature form, then a miniature platform becomes possible, realizing a total weight saving many times greater than the saving in component weight alone.

Fused quartz was chosen very early in the planning for the suspension. Exceptional dimensional stability, ideal elastic properties, and high strength in small cross sections make it an attractive material for this application (Refs. 1 and 2). Techniques already exist (Refs. 1 and 3) for fabricating very small assemblies from fused quartz. The smaller the suspension is made the more rugged it will become, since the strength of fibers increases sharply as they become smaller.

Torsion fibers are the only convenient suspension means which are suited to fabrication from fused quartz, so it may be well to point out a few of the characteristics of torsion suspensions and compare them to the types more familiar in inertial components. The spring rate of

a torsion suspension can be made very small compared to a flexure suspension of the same strength. When one considers the extremely small size into which quartz fibers can be formed, really remarkable uncertainty torque levels can be achieved. In common with flexure suspensions, the torsion element can be made to conduct and used to carry current to the suspended mass, thus eliminating flex leads. These advantages are offset by lack of rigidity perpendicular to the torsion axis and its associated low frequency resonance. The instrument design must provide room for the suspended mass to move, and, very likely, also sufficient damping to control the resonance if operation in a severe vibration environment is contemplated.

The well-known servo force-balance principle has been employed to obtain accurate force readout. In general, this principle utilizes a sensing mass mounted in a suspension so that it is free to move in one direction, but restricted as strongly and rigidly as possible in the plane perpendicular to this direction. Forces applied by the suspension in the direction of free motion, or sensitive axis, are made as small as possible. Any inertial force in the direction of the input axis imposed on the mass is balanced by an electromagnetic force generated by the interaction of an electrical current and a fixed magnetic field. The linear relationship between current and force becomes the means by which acceleration can be accurately read out. Displacement of the mass is sensed

and the forcing current controlled by means of a nulling servo so that the mass remains at a null position with respect to the case of the instrument.

The actual mechanization of the suspension, magnet, and pickoff is shown schematically in Fig. 1. A photoelectric pickoff is almost a necessity because the small mass of the pendulum requires that reaction torques be extremely small. Forces applied to the mass by the position-sensing device will be read out as an error in acceleration. The suspension is of the pendulum type, pivoting about the point at which the torsion fibers attach. The mass is concentrated mostly in a straight cylindrical rod or fiber and is attached to the much smaller torsion fibers by tapered arms, making the whole mass take the form of a horseshoe. The straight section is immersed in the magnetic field, and the entire mass as well as the torsion fibers are made to conduct by an evaporated gold coating. The magnetic field is perpendicular to the length of the straight section of the mass and in the plane of the horseshoe, so the electromagnetic force generated perpendicular to both produces torque about the torsion axis.

This geometry realizes the minimum sensitivity to the position of the current-carrying rod in the field. A uniform field is created between two plane pole pieces, allowing the rod to move in the gap with minimum change of scale factor and also allowing it to tilt with only a cosine relationship to the angle of tilt.

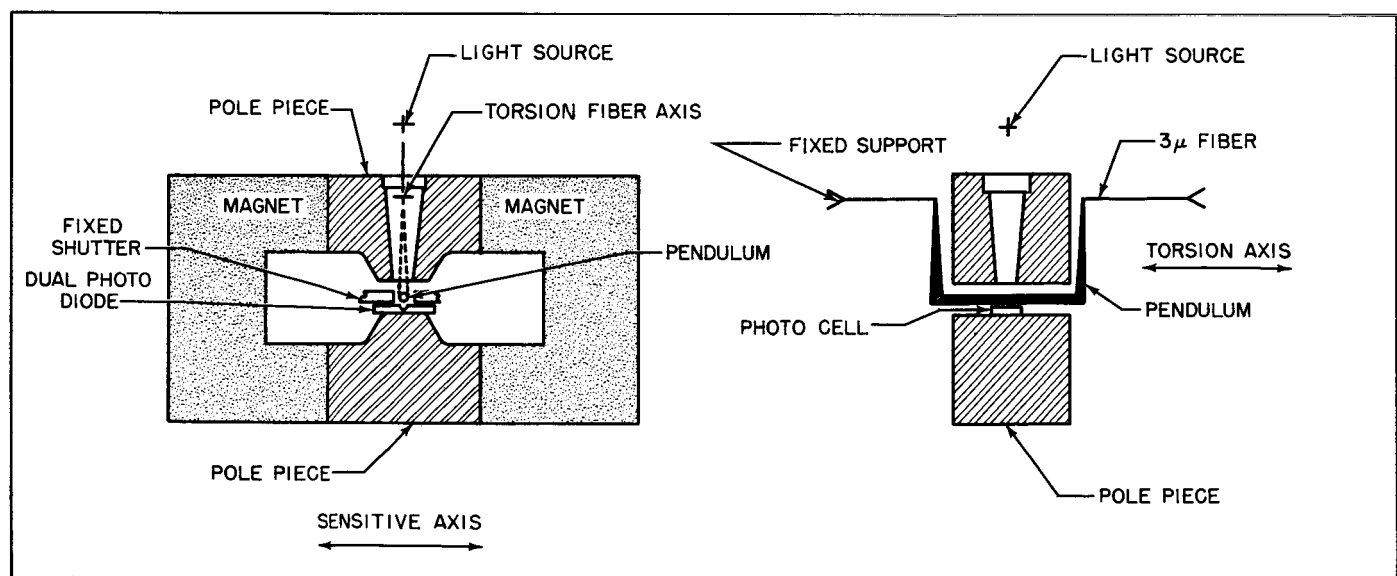


Fig. 1. Diagrammatic View of Accelerometer

The spring restraint obtained is essentially negligible, being very much smaller than in similar instruments using flexure suspensions. With any reasonable degree of stability in the associated electronics, unwanted torques from the suspension will be insignificant in comparison to other uncertainty torques.

One advantage does stem from the characteristic lack of rigidity of the torsion suspension. The mass is contained in a gap and is mechanically surrounded on all sides. There is enough flexibility in the suspension to permit the mass to strike a surrounding part before the torsion fibers are stressed near the breaking point. In other words, the mass is mechanically caged so that it cannot break the weak link in the suspension, the fiber. Since quartz cannot be permanently strained short of actual fracture, the adjustment and subsequent operation of such a suspension should be unaffected by large shocks.

A few comments on the range limitations of the device are in order. First, the current carrying capacity of the torquer is limited since it must enter and leave through an extremely thin gold coating on the microscopic torsion fiber. The current must never exceed the capacity of the fibers or their gold coating would evaporate. The units being tested are scaled for 10 g full scale. Their range cannot be increased without decreasing the size of the mass. Uncertainty torques are expected to remain more or less constant for this type of scaling, so the uncertainty

level in terms of g will increase in proportion to range. An absolute limit set by the practical matter of building a mass and pickoff, only estimated at this point, is in the range of 40 to 100 g .

On the other hand, there is no such limit on the lowest full-scale range that might be realized. The mass may be made as large as desired with the suspension still being protected by the mechanical caging principle. The uncertainty torques, in terms of g , should remain proportional to range if the full current carrying capability of the suspension is used. The only limitation comes from the maximum dc cross acceleration (perpendicular to sensitive axis) which can be sustained without having the mass bottom. Testing in a 1 g field would be possible down to a full scale range of from 0.5 g to 0.05 g . Some testing of a low range suspension is planned.

It is also interesting to note that the accelerometer will make an excellent device to sense level with no special alteration. The low spring restraint and good stability of the suspension make it possible to sense level to an estimated accuracy of about 0.1 second of arc. To do so the accelerometer is mounted as a horizontal pendulum, that is, with the torsion axis vertical, and operated open loop. A magnification of pendulum motion over actual tilt of perhaps three orders of magnitude can be obtained, reducing the effect of pickoff null drift in proportion.

II. DESIGN AND CONSTRUCTION

The accelerometer can be logically broken down into a number of parts, each of which will be discussed separately. The basic element is the suspension. In addition, a magnetic circuit proves the field necessary for torque generation, the pickoff senses motion of the pendulum, and the amplifier completes the servo loop.

A. Suspension

A fused-quartz pendulum, hung by torsion fibers from a supporting structure, makes up the suspension. The supporting structure is also built-up from quartz rod. The whole assembly is an integral piece of fused quartz when completed, ensuring mechanical stability.

An outline of the suspension, including some basic dimensions, is shown in Fig. 2. The 3μ diameter chosen for the torsion fibers is small enough to be difficult to work with without specialized technique, but is larger than

the limiting size ($\approx 1\mu$) for working with micro-torch flames ($1\mu = 0.000040$ inches).

The significant parameters of the suspension are summarized below:

Mass of pendulum	M 0.53 mg
Moment of inertia	J 0.12×10^{-3} gm-cm ²
Pendulosity	P 0.24 dyne-cm/g
Computed torsional spring restraint	k_s 3×10^{-3} dyne-cm/rad
Preload tension	T_0 200 mg

A useful ratio is k_s/P , the ratio of torsional spring restraint to pendulosity, which turns out to be 10^{-2} g/radian, using the figures given above. This ratio gives a measure of the effect of the spring constant on the operation of the accelerometer. It is two to three orders of magnitude smaller than that obtained in other flexure-suspended accelerometers. Any disturbance which can be converted to an equivalent displacement of the mechanical from the electrical null will introduce a null offset proportional to spring constant in a servo force-balance type of accelerometer. The mechanical null is defined as the position of the pendulum at which the spring restoring force of the torsion fibers is zero. The electrical null is defined as the position of the pendulum at which the voltage output of the photoelectric pickoff is zero. Therefore, the null error observed in the torsion fiber accelerometer would not come from the suspension, if the electrical null remains stable within relatively loose limits.

The rigidity of the 10 g suspension to forces applied perpendicular to the torsion fiber and the sensitive axis can also be estimated. Using the numbers given, one obtains 800 dynes/cm⁻¹ for this transverse spring rate. Expressed in terms of g , this means the mass sags 0.006 mm when subjected to 1 g transverse acceleration. If a force is applied in the direction of the torsion fiber instead of perpendicular to it, an angular sag will occur, but the maximum displacement of a point on the pendulum will be of the same order of magnitude. Although more than one would really like to see, displacements of this magnitude do not seem to be prohibitive. The resonance associated with the transverse spring rate is at about 200 cps. Not much can be done to increase it because of limitations imposed by the tensile strength of the fibers, and the square root relationship of frequency to tension.

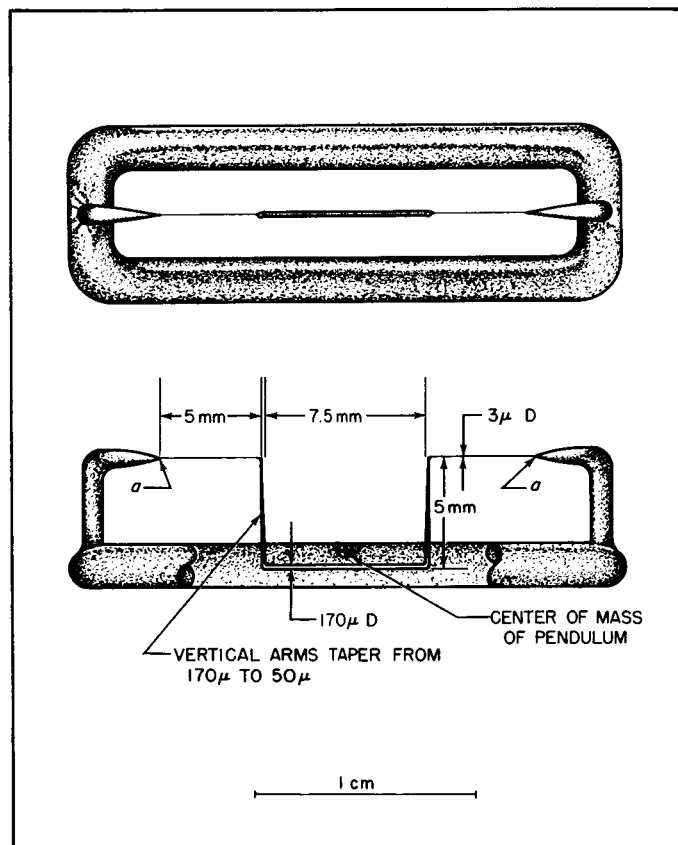


Fig. 2. Fused-Quartz Suspension

As shown in Fig. 2, the mass of the pendulum is fairly well concentrated in the straight rod section located between the pole pieces. If the assumption is made that all the mass is there, then a simple relationship is available to give the pendulum mass as a function of full scale range, R .

$$m \text{ (mg)} = \frac{R}{5} \text{ (g)} \quad (1)$$

A film of gold to carry the torquing current is deposited on the whole suspension by conventional vacuum evaporation techniques. The gold film is broken in two places to provide isolation of the torquer circuit from ground. The rest of the gold merely prevents static charges from building up on the surface of the quartz. The gold film is estimated to be of the order of $1/2\mu$ thick.

The only limitation presented by the gold electrically is on the 3μ fibers themselves. The maximum current

which could be passed through a suspension having a gold coating of thickness such that its resistance was 700 ohms was determined experimentally, at 14 ± 0.5 ma. The total resistance of the two fibers was arbitrarily put at 500Ω in the first suspensions. Since then, lower resistance values have been tried, down to 80Ω , and no bad effects on the elastic properties of the suspension have been observed. Current through the fibers has been limited to 10 ma maximum and no failures have occurred from normal operation. However, transients from ac test equipment can easily exceed 10 ma, and special fuses have been used to protect the suspension. They are made from a short ($1/2$ mm) section of quartz fiber slightly smaller than that used in the suspension. Fuses of 12-14 ma rating and $40\text{-}75 \Omega$ resistance were obtained in this manner.

Two views of a completed suspension are shown in Fig. 3.

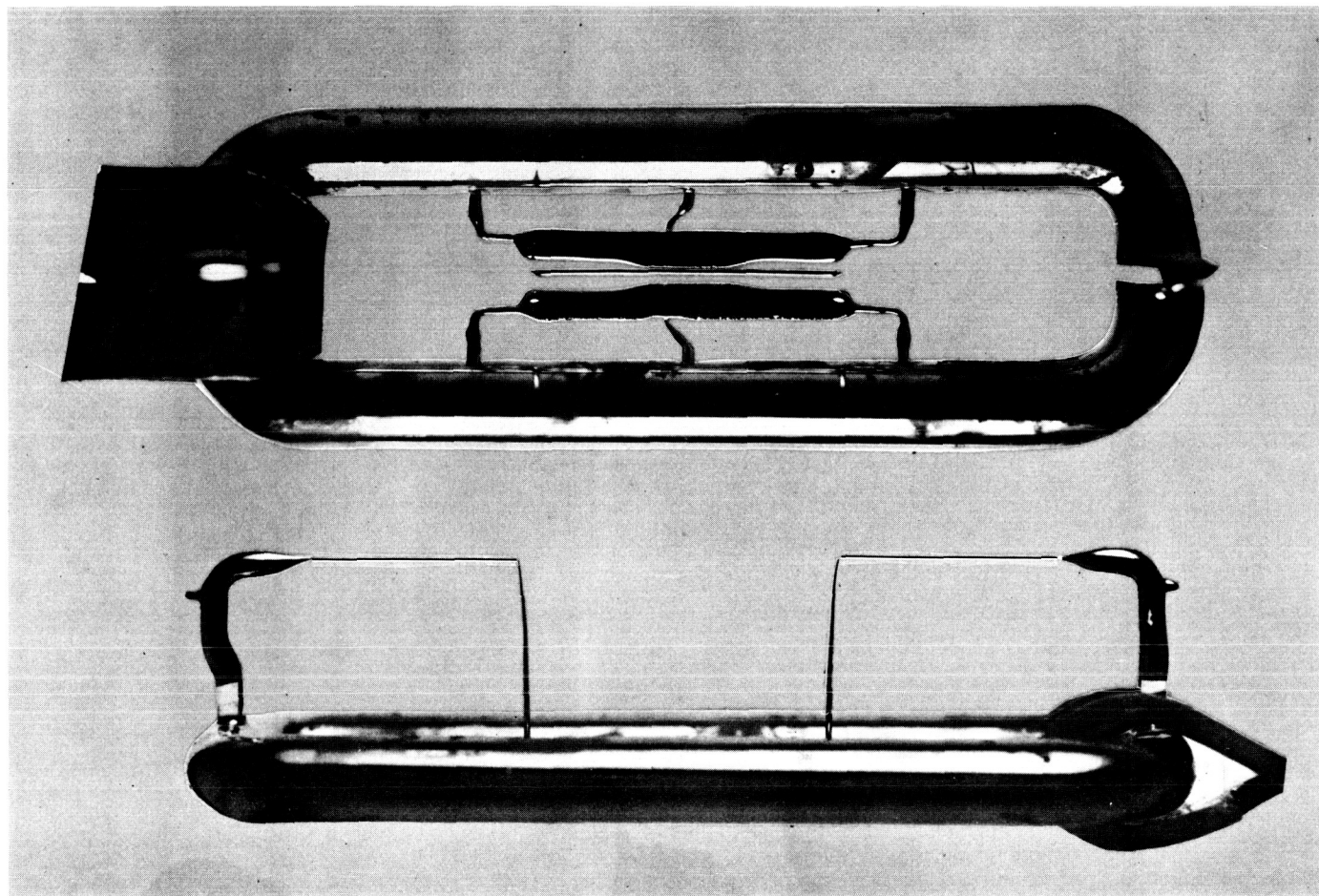


Fig. 3. Two Photographic Views of the Suspension

A few brief remarks on constructing the suspension follow. They are included to give a feeling for the operation rather than as complete instructions for building the suspension. Figure 4 is a view of the working area, showing the microscope, manipulators and torches. The microscope is used both for general observation of the work and for measuring.

The rectangular base of the suspension is built up in a jig, as in Fig. 5. The pointed rods shown in the photograph are used to locate in three dimensions the points to which the torsion fibers are to be fused (the points labelled "a," Fig. 2). Care must be taken when the torsion fibers are mounted that no twist is included, because once the suspension is completed no mechanical adjustments can be made. Another jig is used to locate the pendulum accurately while a flame is passed along the fiber to relieve torsional stress. It appears that bias torque can be held to 3 to 5×10^{-4} g in this manner. Electrical compensation can be employed to eliminate bias of this magnitude without difficulty.

Tension is set into the suspension in the last operation before plating. The top of the fixed support post is fused

to a quartz rod held in a manipulator. The rod is then drawn back by the manipulator while the support post is softened below this point with a flame. The tension is measured by observing the spread of the vertical legs of the pendulum with a microscope.

B. Pickoff

The pickoff used is a dc push-pull photoelectric type employing silicon "solar cell" photodiodes. The operation of the pickoff is illustrated in Fig. 6. The pendulum is placed between two fixed opaque shutters, leaving a narrow gap on each side. The pendulum and shutter arrangement is then illuminated uniformly, perhaps from above. Two separate but identical photodiodes then can detect motion of the pendulum which narrows one gap and widens the other.

The two photodiodes are placed on one wafer of silicon in order to obtain the maximum degree of symmetry. An etched or scribed line through the junction layer of the solar cell serves to separate the diodes. However, the first unit to be tested had two separate photocells. Sym-

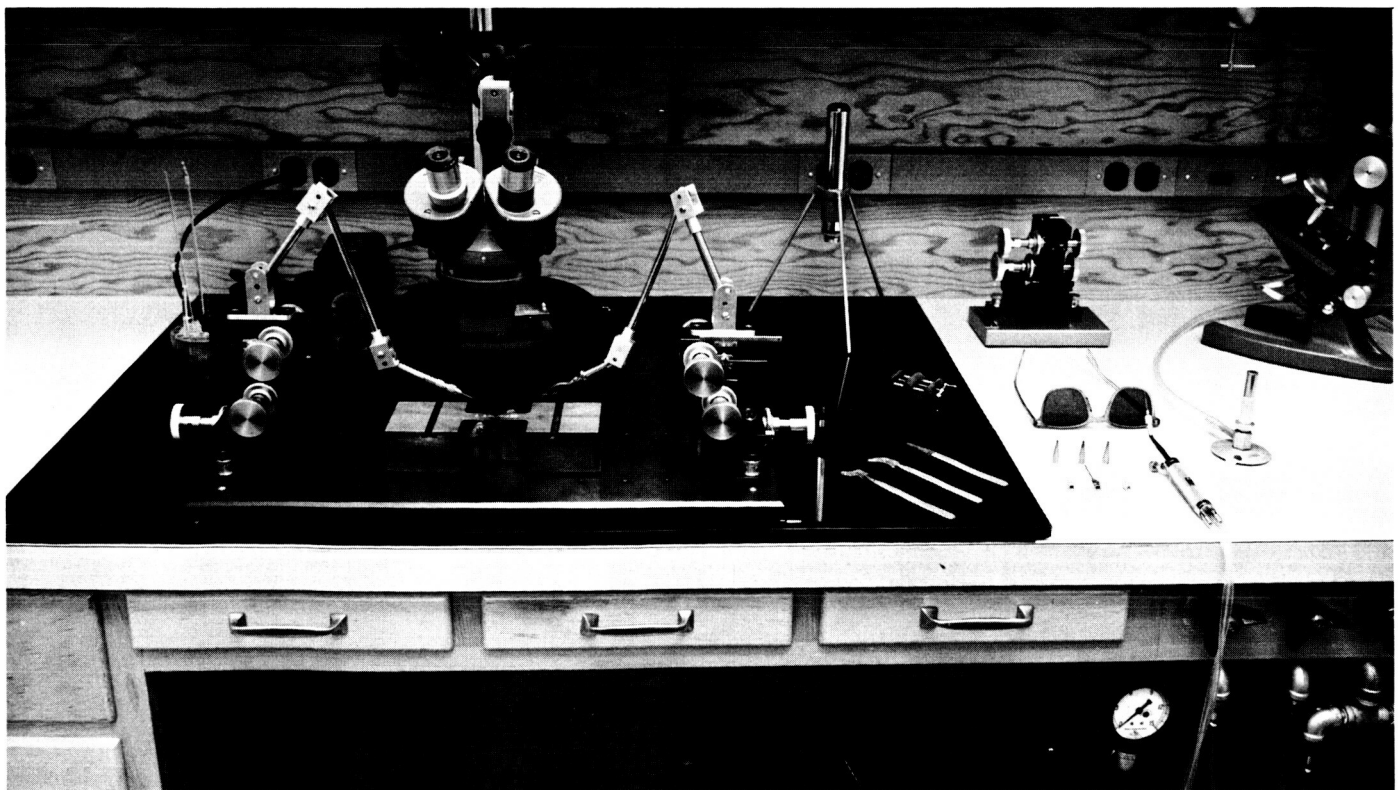


Fig. 4. View of Quartz-Working Area

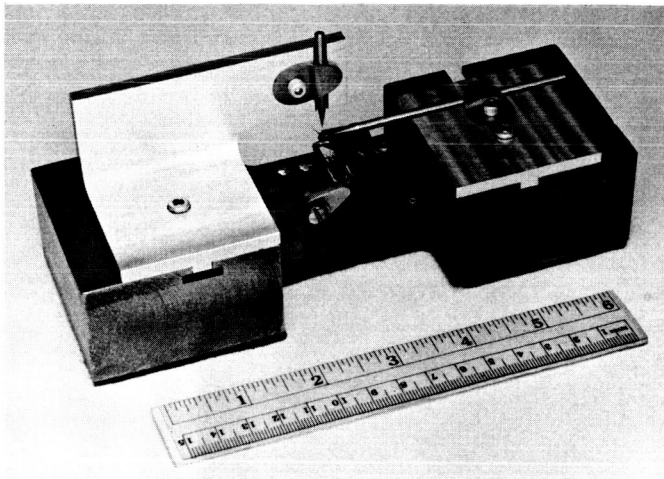


Fig. 5. Suspension Fabrication Jig

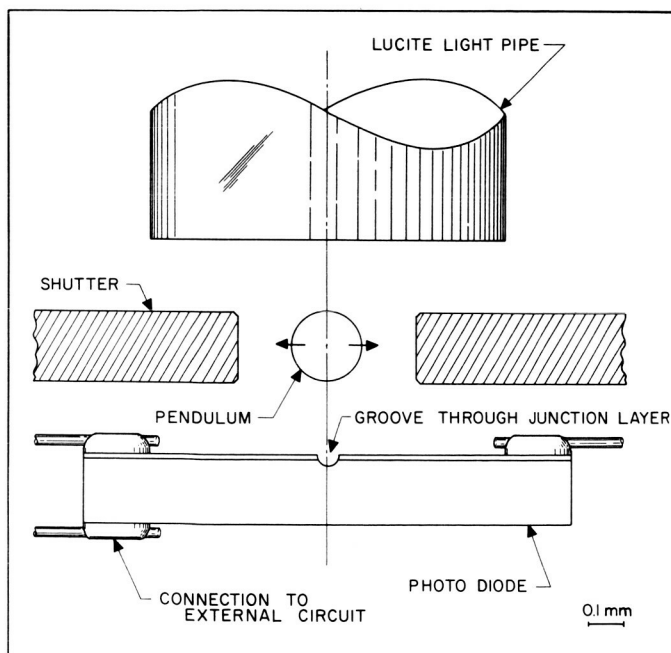


Fig. 6. Diagrammatic View Showing the Pickoff Elements

metry is desirable because it minimizes response to light intensity and temperature variations.

A few of the characteristics of the diodes are as follows.¹

Sensitivity	$8 \mu\text{a f.c.}^{-1} \text{ cm}^{-2}$	Short circuit output current tungsten light
-------------	---	---

Source impedance	30K ohms
------------------	----------

Size (each diode)	$\frac{1}{2} \text{ mm} \times 1 \text{ mm} \times 0.16 \text{ mm}$
-------------------	---

¹Obtained from Electro-Optical Systems, Inc., Pasadena, Calif.

Symmetry, or differences in output between the two diodes on a wafer, was 5% over a two-to-one variation in light intensity, and a temperature range from 75° F to 180° F.

Miniature incandescent lamps were obtained² to excite the pickoff. Their characteristics are as follows:

Diameter	0.100 inch
Length	0.187 inch
Filament rating	3 v, 60 ma

Other miniature lamps are available.³ Most of the accelerometer test data to date has been obtained with the larger ACMI #540-110 lamp. Three of the ACMI lamps and three of similar construction to the CML lamp, but 25% larger, have been shaken at rated voltage to Sergeant type-approval (Ref. 4) and to 36 g noise without failure.

A typical pickoff output curve is shown in Fig. 7. Output current in a 1K load is plotted vs pendulum angle. The ACMI bulb was used.

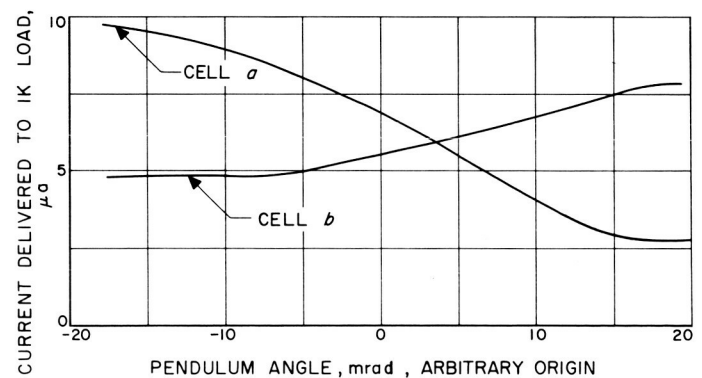


Fig. 7. Output of Pickoff Photodiodes, a and b, as a Function of Pendulum Position

C. Magnetic Circuit

Figure 8 shows the principal dimensions of the magnetic circuit. The magnets are cut from a standard channel horseshoe, of Alnico V alloy. The pole pieces are Allegheny-Ludlum #4750. Charging is accomplished with a commercial impulse charger. The charging current is carried by a silver strap of electrolytic grade 0.030" by 0.180" in cross section, and about 1.00 inch long, which is laid across the throat of each magnet, and carried

²Chicago Miniature Lamp #CM8-666.

³American Cystoscope Makers, Inc.

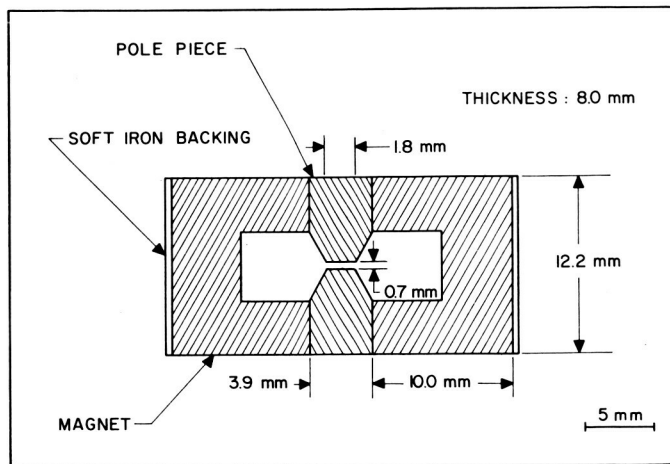


Fig. 8. Sketch of Magnetic Circuit

outside the instrument body along either side of the magnet. The magnet charger had to be altered in order to supply sufficient current because the resistance of the silver straps was larger than it was designed to handle. The $100\ \mu\text{f}$ capacitor in the charger was padded externally with $1000\ \mu\text{f}$, and charged to 450 v. The transformer secondary windings were connected in series rather than parallel, making the step-down ratio 32:1. A field strength of 9000 gauss in the gap has been realized by this procedure.

D. Parts and Assembly

An exploded view showing all the parts is shown in Fig. 9. The assembled instrument is seen in Fig. 10. The

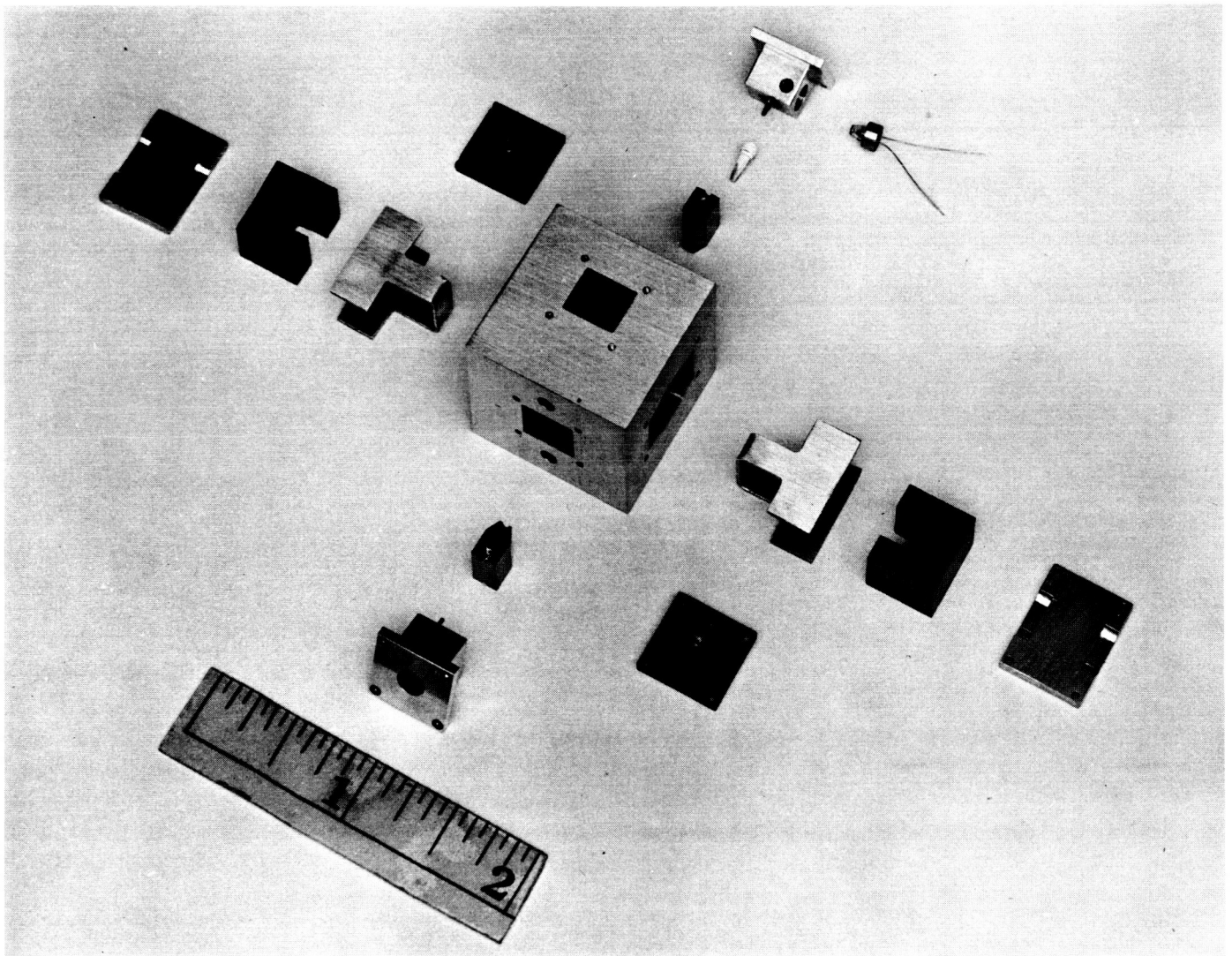


Fig. 9. Exploded View of Mechanical Parts

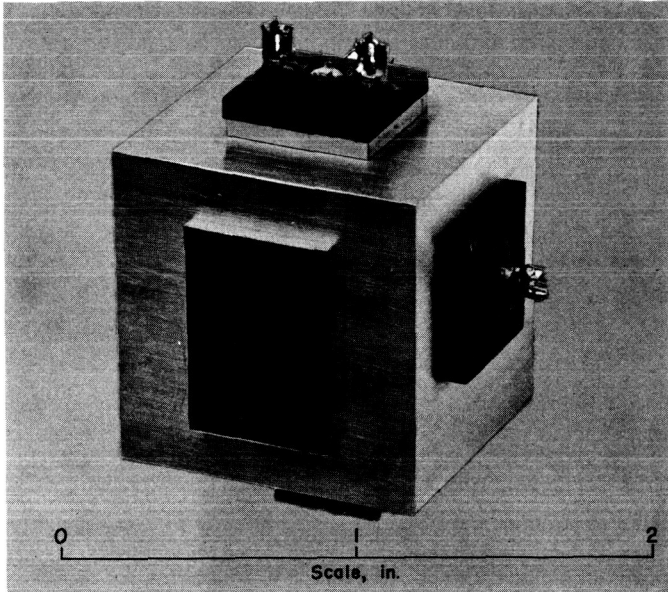


Fig. 10. Assembled Accelerometer

pole pieces, magnets, and suspension are located by the squared holes in the body.

E. Amplifier

Since there is no damping in the accelerometer proper, phase lead must be provided by the amplifier in order to make the servo restoring loop stable. This has been done by placing the proper impedance in the feedback loop of a dc amplifier.

A schematic of the amplifier which was used for ordinary laboratory testing is given in Fig. 11. The push-pull arrangement is used to minimize drift due to temperature changes. The input transistors must be selected for match. They are operated at low base current ($3 \mu\text{a}$) to further reduce drift. With these precautions, it is felt that an equivalent input drift of $\pm 0.2 \mu\text{a}$ while temperature is changed from 75°F to 180°F can be realized in practice.

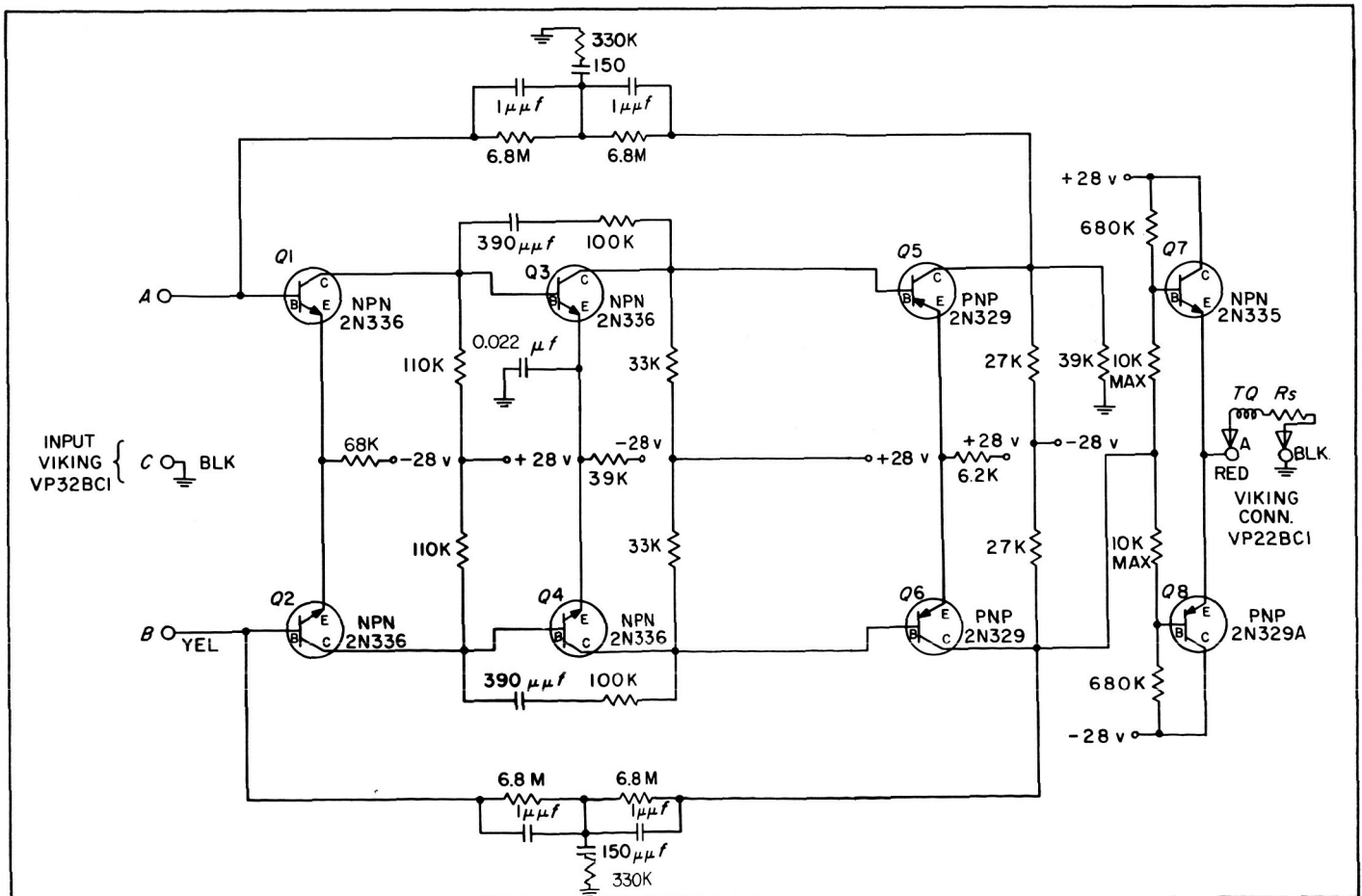


Fig. 11. Schematic of Servo Amplifier Used in Testing

Jet Propulsion Laboratory

Drift of $\pm 0.1 \mu\text{a}$ over the same temperature range has been observed.

The measured gain-frequency curve of the amplifier is shown in Fig. 12. The 330K resistor in the main feedback network was not installed when these curves were taken. The output stage is arranged to saturate at $\pm 10 \text{ v}$ output into 1K load. This limits the current output to 10 ma, so the amplifier cannot accidentally damage the

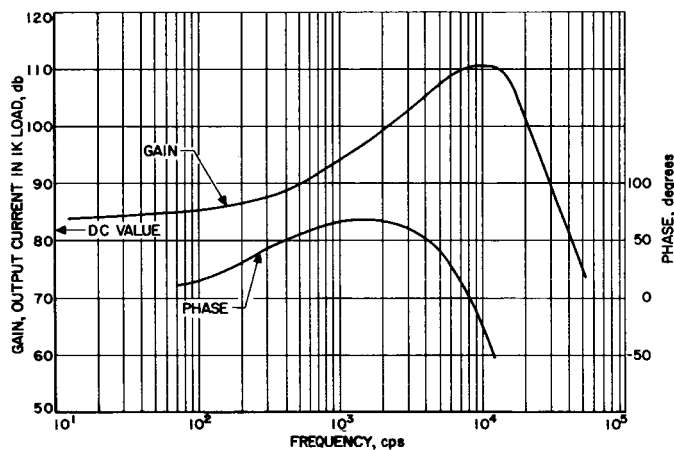


Fig. 12. Experimental Phase and Gain vs Frequency of Amplifier

gold film on the suspension. A drawback of the circuit is that its phase lead is lost if the amplifier saturates. The system is normally stable after a saturating transient; however, trouble has resulted at times. The cure is to take the rate feedback signal out before the last (saturating) stage. The results from the complete accelerometer which follow were obtained with this amplifier.

A block diagram of the force-balance loop is shown in Fig. 13. The parameters shown are the design parameters rather than experimentally measured quantities.

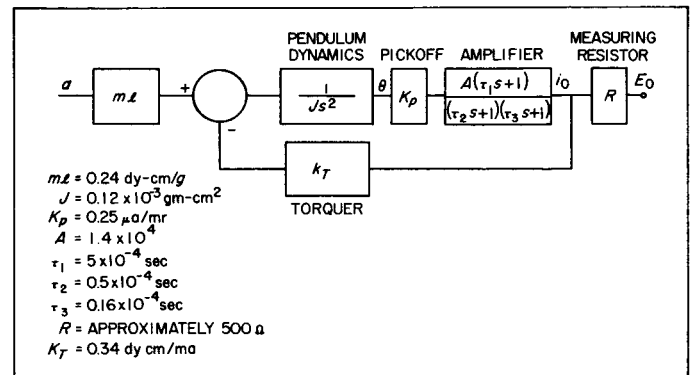


Fig. 13. Block Diagram of the Force Balance Loop, Including Design Parameters

III. EXPERIMENTAL DATA

Many of the tests performed are of a general type which are applicable to any accelerometer, and have been described in more detail elsewhere (Ref. 5). Only a brief description of each test has been included here.

The output current supplied to the load as a function of angular pendulum deflection is plotted in Fig. 14. This curve is obtained by tilting the accelerometer open loop on a dividing head with the torquer replaced in the amplifier output circuit by an equivalent resistor. The orientation is such that the pendulum hangs downward under the influence of gravity. Since the spring rate is small, the rotation of the accelerometer case is equal to the deflection of the pendulum with respect to the case.

The output was lower than the desired 3.5 ma/mr because the output of the pickoff was not as large as expected. It should be possible to increase it by using a more efficient condensing system for the light source. An adjustable preamplifier has been constructed to insert in the loop in front of the amplifier, which can raise the forward gain to the values shown in the block diagram (Fig. 13). The saturation found in Fig. 14 is an amplifier saturation and is not the mass hitting the stops.

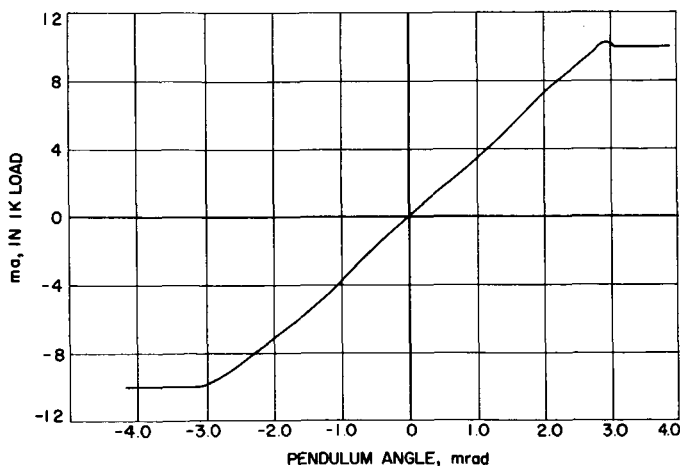


Fig. 14. Output Current From Amplifier in 1K Load vs Pendulum Angle, Open Loop

A general stability test is used to determine scale factor, null offset, and null angle of the operating accelerometer. The accelerometer is oriented by means of a dividing head at four positions separated by 90° . In two

of the positions, the accelerometer is sensing nearly zero g ($\theta = 0^\circ$ and 180°), and in the other two, plus or minus one g ($\theta = 90^\circ$ and 270°) respectively. The torsion axis of the accelerometer is placed parallel to the dividing head axis.

θ = Dividing head reading

$E_0(\theta)$ = Accelerometer output voltage

N_0 = Null offset, $0/180$

N_a = Null angle

k_1 = Scale factor

Then:

$$k_1 = \frac{1}{2} [E_0(90^\circ) - E_0(270^\circ)] \quad (\text{Scale factor})$$

$$N_0 = \frac{E_0(0^\circ) + E_0(180^\circ)}{2k_1} \quad (\text{Null offset})$$

$$N_a = \frac{E_0(0^\circ) - E_0(180^\circ)}{2k_1} \quad (\text{Null angle})$$

Null offset is defined as the output of the accelerometer when the input acceleration is zero. Null angle is the angle between the sensitive axis and a reference fixed in the case of the instrument. The reference is arbitrary, remaining fixed only for the duration of one test. If the accelerometer is dismounted, or a new dividing head zero is chosen, then a new null angle reference will result.

The test just described is also convenient to use in obtaining the dependence of these three parameters on other variables, such as temperature and supply voltages.

To date, three suspensions similar to the one shown in Fig. 3 have been tested, using two sets of metal parts. The null offset on two of the units averaged $10.4 \pm 0.5 \times 10^{-4} g$ and $2.9 \pm 0.5 \times 10^{-4} g$ respectively. These averages were taken over the entire period of testing, which was several weeks for each suspension. All determinations in which the accelerometer was being operated in its normal configuration were included. It is possible to buck out an average offset of this order of magnitude electrically to sufficient accuracy that the measured uncertainty represents the instrumental accuracy. No null torque compensation has been employed in the tests to date. The experimental null uncertainty, or variation of null offset, is therefore approximately $\pm \frac{1}{2} \times 10^{-4} g$ over a period of several weeks.

The third suspension had a very high null offset ($130 \times 10^{-4} g$) and high spring constant. The reason for this has not yet been determined. Except for the high null torque, its performance has been satisfactory.

The uncertainty in scale factor, null offset, and null angle over a short period of time, approximately one hour, are given below, where all tests on the two good suspensions are averaged. (1σ values from six tests were averaged arithmetically.)

$$\frac{\delta K_1}{K_1} = \pm 0.3 \times 10^{-4}$$

$$\delta N_0 = \pm 0.5 \times 10^{-4} g$$

$$\delta N_a = \pm 0.6 \times 10^{-4} \text{ rad.}$$

A set of data is included in Table 1 as an example. These data show slightly better stability than the average, as can be seen by comparing the δ values to the ones shown above. Note that a null offset can also be obtained from $E_0(90^\circ) + E_0(270^\circ)$. This in general varies from the 0° to 180° value, and the difference is an indication of the nonlinearity to be expected. For the data shown, the difference is $0.42 \times 10^{-4} g$.

If the pickoff null is moved intentionally, the dependence of null offset and scale factor on pendulum position is obtained. The results of such a test are plotted in Fig. 15. Provision is made in a special preamplifier for shifting the null position to cover the complete range between stops if desired. The slope of the null offset

vs null angle is, of course, the spring constant. The measured value is $0.06 g/\text{rad}$ compared to the expected value of $0.01 g/\text{rad}$. The reason for the difference is not yet completely clear, although one would at first suspect that the fiber diameter is larger than normal. However, $0.06 g/\text{rad}$ is still small enough that it presents no difficulty. The scale factor curve is actually a measure of the dependence of the magnetic field on position in the gap. The fact that the minimum of the scale factor curve is not centered indicates that the normal (unbiased) pickoff null position is not centered over the poleface, or that the polefaces are not parallel.

The variation of null angle and scale factor with temperature are given in Fig. 16. The scale factor change merely reflects the variation of strength of the Alnico V permanent magnets with temperature. No compensation was employed. The scale factor could be made fairly independent of temperature by placing a thermistor on the magnet, which electrically shunts the measuring resistor—a technique which has been applied successfully in other permanent magnet accelerometers.

The measured null angle will change with temperature because of drifts in the pickoff or electronics. It is unequal changes in the pickoff photodiode outputs which caused the drift, since the amplifier was not in the oven during the temperature test. However, it now appears that the amplifier will not be a significant cause of null angle drift even if it also were temperature-cycled. It should be possible to significantly improve this characteristic by improving technique for making the photocell, as described earlier, and by improved condensing

Table 1. Accelerometer Stability Test

Trial No.	$E_0 \theta=0$ volts	$E_0 \theta=90$ volts	$E_0 \theta=180$ volts	$E_0 \theta=270$ volts	Scale Factor volts/g	Null Offset g	Null Angle radians
1	0.000000	0.835094	0.001815	0.833236	0.834165	0.001088	-0.001088
2	0.000016	0.835162	0.001837	0.833239	0.834200	0.001091	-0.001107
3	0.000034	0.835154	0.001803	0.833246	0.834200	0.001060	-0.001094
4	0.000000	0.835091	0.001824	0.833259	0.834175	0.001093	-0.001093
5	0.000055	0.835098	0.001834	0.833257	0.834178	0.001066	-0.001011
Average					0.834184	0.001080	-0.001079
1σ deviation for one trial					± 0.000014	± 0.000014	± 0.000034

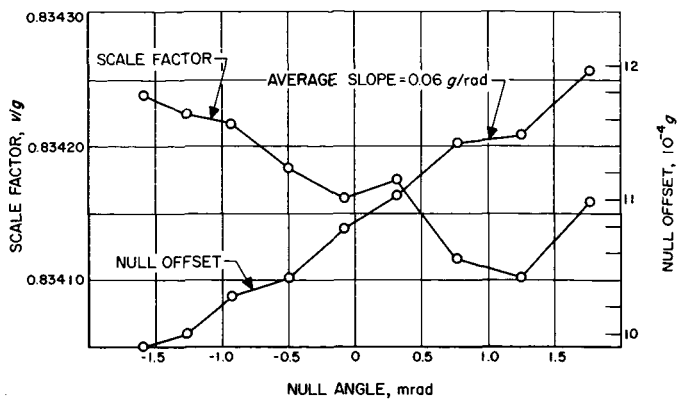


Fig. 15. Null Offset and Scale Factor as Function of Null Angle

optics. The pickoff used for the data shown had two separate cells mounted adjacent to each other instead of the dual cell.

This pickoff has also been found sensitive to light bulb voltage. Ten percent change in lamp voltages produced one milliradian null angle change. No difficulty has been encountered in testing because of this. Work directed toward reducing the effect is in progress.

The results from a 1 g linearity test on suspensions No. 1 and No. 2 are shown in Fig. 17. The accelerometer

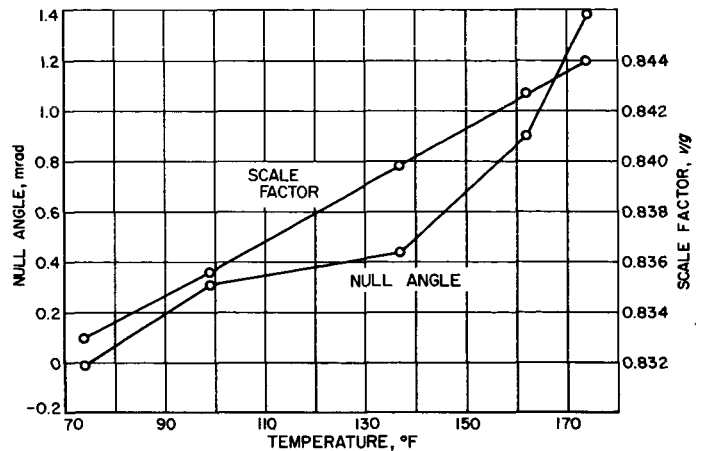


Fig. 16. Null Angle and Scale Factor as Function of Temperature, for Elevated Temperature

was mounted on a dividing head with the torsion axis perpendicular to the dividing head axis to eliminate cross-coupling errors. The servo constraint was low ($\sim \frac{1}{2}$ mr/g) for these tests because of low magnetic field and low pickoff output. The quantity plotted is δ_a vs applied acceleration, where:

$$\delta_a = k_1 E_o(\theta) - A_i(\theta) - N_0$$

where

$$A_i(\theta) = g \sin(\theta), \text{ applied acceleration}$$

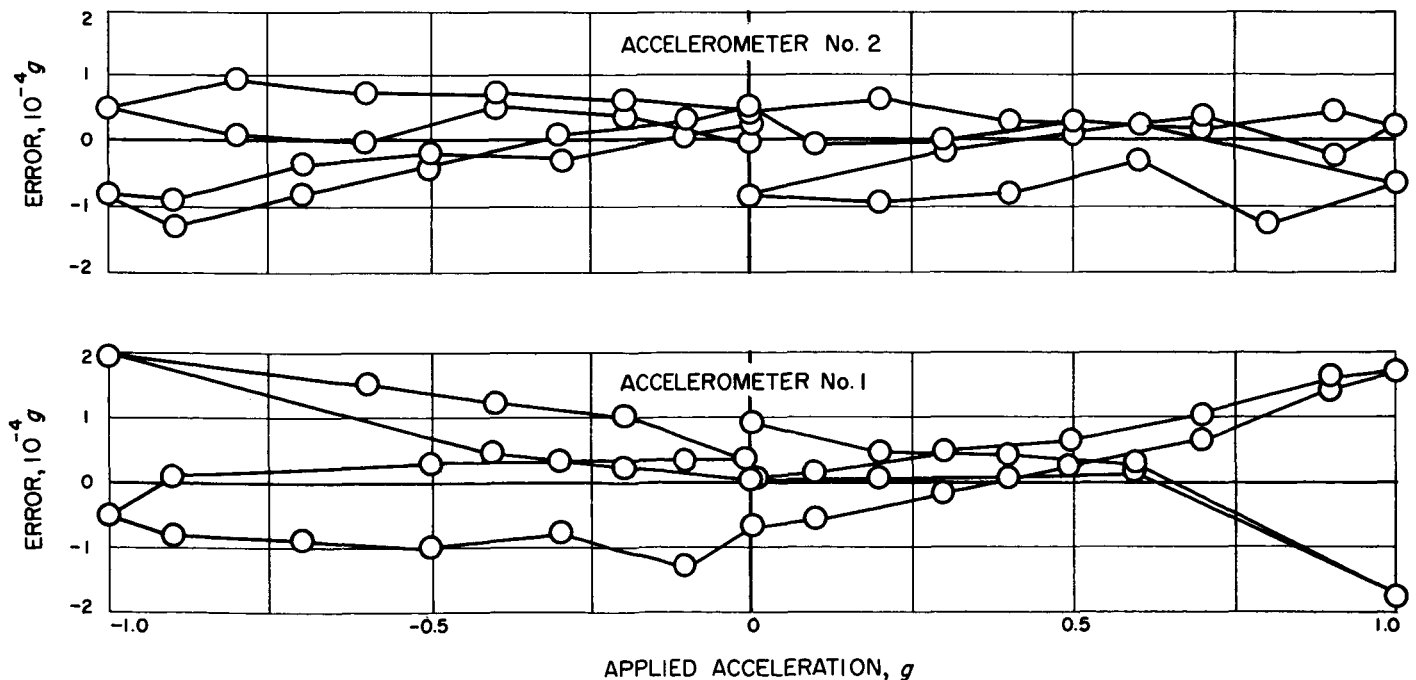


Fig. 17. 1 g Linearity Test of Two Suspensions

δ_a = acceleration error, in g

k_1 = scale factor, determined from data

$E_o(\theta)$ = accelerometer output

N_o = null offset

θ = dividing head reading, measured from the angle which places the sensitive axis horizontal

g = local acceleration of gravity

The rms 1σ error obtained for δ_a in the two suspensions was $0.86 \times 10^{-4} g$ and $0.57 \times 10^{-4} g$ respectively.

Two units were tested above 1 g on a centrifuge instrumented by JPL. The results were in agreement. The data for the second test is presented in Fig. 18. The input acceleration was taken up to 10 g in both + and - directions. The scale factor k_1 in arbitrary units is plotted against acceleration. Its slope is approximately $+\frac{1}{2} \times 10^{-4}$ per g . This result is similar to that obtained with other accelerometers on the same centrifuge. The lack of closure of the data for plus inputs is possibly instrumental. The droop in the curve at low g levels is instrumental and is characteristic of data from the centrifuge.

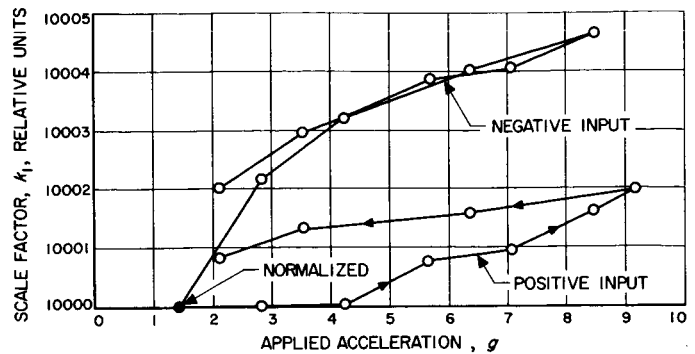


Fig. 18. Data From Centrifuge Test

The frequency response of the accelerometer was measured by injecting an ac electrical current into the torquer. Such an input looks like an acceleration input to the accelerometer, and the results correlate well with an actual sinusoidal acceleration input obtained from a shake table. With gains approximately in accordance with Fig. 13, -3db occurred at approximately 650 cps. Sharp peaks occur at 750 cps and 12 kc; the first, a resonance of the mass of the tapered arms of the pendulum and the stretched fibers; and the second, probably the fundamental mode of the fibers themselves. Both peaks can be eliminated by introducing damping.

IV. CONCLUSIONS

To date, the tests of the miniature accelerometer have demonstrated that it is feasible to build a small suspension from fused quartz which has very small uncertainty torques—that is, small in comparison to the pendulosity of the suspended mass. The good stability that one would expect to find in quartz was found to exist experimentally over at least the two months' testing period of one of the accelerometers. No uncertainty torque that could be laid with certainty to the suspension was observed. Of course, it is difficult to separate the several causes of null torque, but the fact that its long-term uncertainty was no worse than the short term tends to rule out an effect such as creep which occurs over an extended period. A random effect such as convection currents in the air surrounding the mass seems a more likely cause. It is possible to conclude that the mechanical uncertainty torque must be less than the observed 0.5×10^{-4} g null uncertainty.

Because the suspension fibers and the mass have been made extremely small, the uncertainty torques are much smaller in an absolute sense than those familiar to the component field. A null uncertainty of 10^{-4} g corresponds to a torque of 0.25×10^{-4} dyne-cm, or 0.05 microgram-weight, expressed as a force. The maximum measurable torque is 2.5 dyne-cm, or approximately 1 milligram-weight, as a force.

It proved possible to build a serviceable pickoff free of reaction torques using photoelectric techniques. A special detector was developed, and dc electronics were used. Such an arrangement should not be expected to show exceptional null angle stability, but the low spring restraint of the suspension enables a reasonable null angle shift to be tolerated without an accompanying null torque change. Errors caused by null angle change can be minimized by proper orientation of the accelerometer in a missile. Short term null angle shifts of 0.05 milliradian, and temperature-induced shifts of 1 to 2 milliradians were observed, but improvement of the latter should be possible. No really long term tests have yet been made.

No shake test results have been included, as tests are still in progress. It now appears that damping of the low frequency resonance of the suspension will be necessary to prevent the mass from striking the pole-pieces. The maximum vibration level under which the accelerometer still operates will be determined, and the rectification

resulting from operation in a vibration environment will be measured. Preliminary indications are that the principle of mechanically caging the mass will be effective. One accelerometer has been shaken at 18 g rms noise (20-1500 cps) on all three axes without a permanent change (after shaking) in null offset exceeding 1×10^{-4} g.

If accurate performance under vibration environment proves to be a limiting factor, the well-known techniques of fluid-damped or floated components are of course available for use with this type of suspension. It should be emphasized that the vibration problem is one of having the accelerometer operate to specification in a severe vibration environment. The present units survive severe vibration without any significant changes in their characteristics.

No attempt has been made to package either the accelerometer proper or the electronics in the minimum possible space. The weight and volume of the accelerometer is chiefly in the magnetic circuit, but it should still be possible to package it in one-half of the present volume, using the same suspension and magnetic field.

A recurring problem with fused quartz is the difficulty of procuring fused-quartz assemblies. This should not always be the controlling consideration in its use. The techniques used, although unfamiliar, are no more difficult than the high precision machine-shop techniques ordinarily used for precision components. The suspensions described have been made successfully at JPL without previous experience in the practical problem of working fused quartz. The technique had to be learned by the instrument specialist who performed the work as he went along. Three firms have also undertaken to supply an experimental suspension (not all like this one) with varying degrees of success. A period of trial-and-error learning may be necessary for each of them. It would probably be easier to purchase a larger number of suspensions (say 25 or more) of the same design, since the lessons learned on the first ones could become profitable later. More time could also be spent on production technique.

Work is continuing in an effort to introduce damping into the suspension in order to control its transverse resonance, and to improve the sensitivity and gain of the pickoff. Three complete accelerometers are now being assembled. They will be put through a comprehensive series of tests.

REFERENCES

1. Strong, J., *Procedures in Experimental Physics*, chapter VI, by H. V. Neher, Prentice-Hall, Inc., New York, New York, 1938.
2. Tighe, Nancy J., *Fused-Quartz Fibers*, National Bureau of Standards Circular 569, January 25, 1956.
3. *Drawings and Working Quartz Fibers*, Argonne National Laboratory, Chicago, Illinois, March, 1946.
4. Jacobson, N. F., *Jet Propulsion Laboratory Environmental Testing Specification, Flight Equipment*, No. 14803, Paragraph 6.5.1.1, Jet Propulsion Laboratory, Pasadena, California, May 26, 1959.
5. *Accelerometer Testing Procedures*, Jet Propulsion Laboratory Technical Document 12-25-6, Jet Propulsion Laboratory, Pasadena, California, September 20, 1957.

ACKNOWLEDGMENTS

A great deal of appreciation is due W. H. Hermann, whose facility with the many new techniques involved helped to surmount many difficulties. His skill with the fused-quartz fabrication was indispensable. Thanks are

also due to E. Bates for much of the assembly work, and to H. Ailslieger for the testing.

The basic concept for the dc amplifier is due to Dean Slaughter.